Flow Field Effect on Electric Double Layer during Streaming Potential Measurements

Fuzhi Lu, Jun Yang, and Daniel Y. Kwok*

Nanoscale Technology and Engineering Laboratory, Department of Mechanical Engineering, University of Alberta, Edmonton, AB T6G 2G8, Canada

Received: April 20, 2004; In Final Form: July 13, 2004

It is typically assumed that flow field has very little or no effect on the electric double layer distribution. Here, we study this effect by means of a dilute electrolyte (deionized water) in a streaming potential mode for a 40-μm parallel-plate microchannel. By measuring the electrical potential downstream along the channel surface, we have shown that the potential distribution along a streamwise direction can be nonlinear. By means of a current continuity equation, we also presented numerical simulation results of potential distribution for pressure-driven flow with electrokinetic effects. The simulated results agree well with those from experiment. Results indicate that the conduction current in the streamwise direction is only a fraction of the streaming current. As a result, the ζ-potential values determined from streaming potential measurements are generally smaller than those from streaming current measurements. It is expected that this discrepancy would be smaller for a more concentrated electrolyte.

I. Introduction

The concept of an electric double layer (EDL) and the equations for electrokinetics were originally formulated by Helmholtz. The static EDL theory of Helmholtz,[1] which was later developed by Gouy[2] and Stern,[3] has been employed to streaming potential studies for decades. The applicability of the static EDL theory to systems composed of solid surface and aqueous solutions of electrolytes has been challenged by experiments with single capillaries as well as porous plugs. It was found that ζ-potential values for a given interface calculated from streaming potential measurements do not agree with those from electroosmotic and electrophoretic studies.[4−8] A variety of experiments, however, showed that ζ-potential values for a given interface when calculated from electrophoretic, electroosmotic, and streaming potential measurements can be identical.[4,5,9]

Another method of testing the static EDL theory as applied to streaming potential is to compare whether the ζ-potential values determined from the streaming potential and the streaming current method are identical. It has been found that the absolute values of the apparent ζ-potential determined from the latter are generally higher than those from the former.[10−12] Typically, the ζ-potential values from the streaming potential are adjusted to be the same as those from the streaming current method by varying the surface conductance. Even with this "correction", a small but nonnegligible scatter can still be observed in the ζ-potential determined for capillaries of different diameters.[12] The difficulty of this approach is that surface conductivity cannot be easily measurable since it depends on the size of the capillary and the property of an interface. Some authors indeed have employed this method to calculate surface conductivity.[11,13] The static EDL theory when applied to streaming potential measurements fails to explain the substantial decrease in ζ-potential when capillary size decreases and this was first demonstrated by White and Bull et al.[14,15] By correction through surface conductance, these discrepancies appear to be explained satisfactorily. However, we wish to point out that, as surface conductance is a dependent variable and cannot be measured independently, adjustment of this property to compensate for the discrepancy in ζ-potential may imply variation of a property that might not truly reflect physical reality. This approach has also been employed to derive surface conductivity.[12,16]

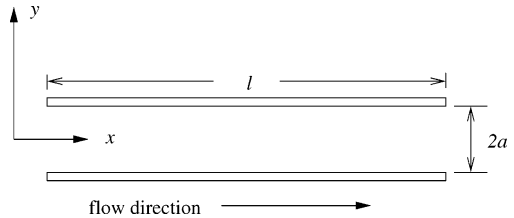

Figure 1. Coordinate system for a parallel-plate microchannel system where l and $2a$ are the channel length and height, respectively.

Other than the above experimental approaches, a number of papers have been published recently regarding the various computational methods to electrokinetic flows based on a decoupled approach, i.e., the ion distribution near the EDL is unaffected by its velocity flow field. That is, given the geometry in Figure 1, the decoupled approach yields the total potential at a point (x, y) in a channel as

$$\phi = \phi(x, y) = \psi(y) + [\phi_0 - xE_x] \tag{1}$$

where $\psi(y)$ is the potential due to double layer at a static state with no fluid motion and no applied external field, ϕ_0 is an imposed potential, and E_x is an electric field (assumed to be constant). Equation 1 assumes that there is no effect of the velocity flow field on the EDL. By superposition of the two potential distributions, Patankar and Hu[17] modeled electroosmotic flow (EOF) in channel junctions using a finite volume approach in three-dimensional channels. Their idea was based on the linearized Poisson−Boltzmann (LPB) equation that can be solved numerically first for the charge distributions along

* To whom correspondence should be addressed. Phone: (780) 492-2791. Fax: (780) 492-2200. E-mail: daniel.y.kwok@ualberta.ca.

10.1021/jp048277z CCC: $27.50
Published on Web 08/27/2004

the wall. The external electric field that induces the electric body force can then be obtained by solving a Laplace equation with a properly imposed potential difference. The exact Poisson−Boltzmann (PB) equation has also been employed by Hu et al.[18] based on a similar approach. Ermakov et al.[19] hypothesized that the effect of the EDL can be represented by replacing the no-slip condition at the channel wall with an analytical formulation of EOF velocity. A "finite cloud algorithm" method was used by Mitchell et al.[20] to compute a steady flow in various channel junctions. A "layer model" was developed by MacInnes[21] for electrokinetic reacting flow where chemical reaction plays a prominent role. However, in geometries where the characteristic dimensions are comparable to the Debye length, these decoupled potential approaches are no longer valid as the flow field effect on EDL structure becomes much larger. For this reason, Yang et al. and van Theemsche et al.[22,23] proposed a general model that is more valid in such geometries to simulate electrokinetic flow in slit channels. It should be pointed out that this model does not employ the Poisson−Boltzmann equation to govern the electric potential and charge density distribution in EDL. Their numerical simulations, however, are limited to a small length-to-height ratio due to large computational effort. Thus, comparison of such numerical results to experimental data directly is difficult.

In the present work, we study experimentally the effect of flow field on the EDL during streaming potential measurements. The electric potentials in the streamwise direction are measured for pressure-driven liquid flow in a parallel-plate microchannel. By checking their linearity, one may deduce the extent of flow field effect on the double layer in the streaming potential mode. The electric potential distribution is also simulated by numerical solution of the governing equations similar to those by Yang et al. and van Theemsche et al.[22,23] but with an assumption of constant liquid conductivity. This assumption allows us to compare the simulated results directly with those from experiments. Instead of the general convection−diffusion−migration equation, a current continuity equation for the distribution of ions is employed here to govern the flux of ion species through the microchannels. The requirement of current continuity has recently been emphasized for heterogeneous microchannels.[24] By solving the established governing equations for pressure-driven flow with a finite-volume-based solver in different boundary conditions, we present the electrical field distribution in EDL and compare that with our experimental results. It will be shown experimentally and theoretically that the potential distribution in the EDL along a streamwise direction for a parallel-plate microchannel can be nonlinear.

II. Theory

A. The Classical Equations for Pressure-Driven Flow. We start by discussing the classical theory from Helmholtz. Helmholtz[1] assumed that there is an immobile layer of electric charges on a solid at the solid−liquid interface, and another mobile layer of opposite charges in the liquid. If the solid is held in position while the liquid passes through, the movement of liquid will cause a potential gradient in the streaming direction that is known as the streaming potential gradient. The total potential that builds up in the direction of streaming in this manner is the streaming potential. It was later realized that the solution layer must be diffused; the charge and electrical potential distributions can be obtained by solving the Poisson−Boltzmann equation. On the basis of the theory of Helmholtz, the streaming current I_s created by continual transfer of electricity as liquid flows will be balanced by a back current I_c caused by the streaming potential and liquid conductivity. The equilibrium state is characterized by a zero net current through the channel:[25]

$$I_s + I_c = 0 \tag{2}$$

Equation 2 implies that both I_s and I_c are in the streamwise direction and Boltzmann distribution remains valid with the introduction of a flow field. In other words, the conduction current in the y direction is assumed to equilibrate exactly by the diffusion current in the same direction. In fact, the Boltzmann distribution can be derived from the balance between diffusion and conduction currents.[21] Assuming the specific conductivity of liquid and surface to be constant in the streaming direction, and if there is no path other than that through the liquid and the surface by which I_c may pass, the electric potential distribution along the streamwise direction should be linear as given by Ohm's law. The total potential at a point (x, y) in Figure 1 will be a superposition of EDL and streaming potentials. If we neglect the difference between surface potential and ζ-potential (ζ), the measured electric potentials $\phi_{sf}(x)$ near the solid−liquid interface are the superposition of the potential in the bulk $\phi_B(x)$ and ζ-potential (ζ) given by

$$\phi_{sf}(x) = \phi_B(x) + \zeta = -\frac{I_c}{K_b + K_s}x + \zeta = \frac{\phi_s}{l}x + \zeta \tag{3}$$

where K_b and K_s are the specific conductivity of the bulk liquid and surface, respectively, and ϕ_s is the streaming potential across the two ends with a channel length l. According to eq 3, the potential distribution in the streaming direction will be linear with a constant electric field E_x ($E_x = \phi_s/l$).

B. Numerical Method. *1. Electrokinetic Equations.* Here, we describe a more general approach without the use of the Poisson−Boltzmann equation and a prior assumption of the electric field distribution, i.e., eq 3. The electric field in a dielectric which carries free charges is governed by the Poisson equation. It is assumed that magnetic field, either applied or induced by current flow, may be neglected. The Poisson equation is given by

$$\nabla\cdot(\epsilon\nabla\phi) = -\rho_e \tag{4}$$

where ρ_e is the net charge density, ϵ is the permittivity of the medium, and ϕ is the electric potential. The net charge density ρ_e can be expressed in terms of species molar concentration c_i as

$$\rho_e = F\sum^{i} Z_i c_i \tag{5}$$

where F is the Faraday constant and Z_i is the valence of species i. Assuming that the flow is dominated by the solvent, the species concentrations for dilute solutions are governed by the general convection−diffusion−migration equation:[21]

$$\frac{\partial c_i}{\partial t} = -R_i - \nabla\cdot(\vec{v}c_i) + Z_i\mu_i F\nabla\cdot(c_i\nabla\phi) + D_i\nabla^2 c_i \tag{6}$$

Equation 6 expresses the flux of each species i in the solution due to convection of the solvent, diffusion, and migration if the reaction rate is set to zero, $\vec{v}$ is the fluid velocity, D_i represents the diffusivity, μ_i is the ion-mobility, and R_i is the reaction rate. In addition to viscous and pressure stresses, the species in the liquid and the liquid itself are subjected to an electric force. Together with the mass continuity equation, the

pressure and velocity field can be described by the following incompressible Navier−Stokes equations

$$\frac{\partial \rho \vec{v}}{\partial t} + \rho \vec{v} \cdot \nabla \vec{v} = -\nabla p - \rho_e \nabla \phi + \mu \nabla^2 \vec{v} \tag{7}$$

$$\nabla \cdot \vec{v} = 0 \tag{8}$$

where p, ρ, and μ are the pressure, density, and viscosity of the liquid, respectively. We have assumed the liquid density to be uniform as its variation caused by the difference in pressure and temperature is negligible. If charge is transferred in the liquid only by movement of ions, the charge distribution is determined by solving the species transport eq 6. The summation over all species of the product of species charge gives the charge continuity equation

$$\frac{\partial \rho_e}{\partial t} + \nabla \cdot \vec{\imath} = 0 \tag{9}$$

where $\vec{\imath}$ is the electric current flux given by

$$\vec{\imath} = \sum^{i} Z_i F \left(-D_i \nabla c_i + \vec{v} c_i - \frac{Z_i F D_i c_i}{RT} \nabla \phi \right) \tag{10}$$

For electroneutral and uniform solutions, the first two terms on the right-hand side vanish. In this case, Ohm's law between current flux and potential gradient applies

$$\vec{\imath} = -\sum^{i} \frac{Z_i^2 F^2 D_i c_i}{RT} \nabla \phi = -\sigma \nabla \phi \tag{11}$$

where σ is the conductivity of the solution defined as

$$\sigma = \sum^{i} \frac{Z_i^2 F^2 D_i c_i}{RT} \tag{12}$$

For the case of equal species diffusivity $D_i = D$, the current continuity equation can be written as

$$\nabla \cdot \vec{\imath} = -D \nabla^2 \rho_e - \nabla \cdot (\sigma \nabla \phi) + \nabla \cdot (\rho_e \vec{v}) = 0 \tag{13}$$

By solving the set of eqs 4, 6, 7, and 8 simultaneously with the appropriate boundary conditions, one obtains the distribution of $\vec{v}$, ϕ, and c_i. However, direct numerical simulation would require considerable computational effort to ensure adequate accuracy over the double-layer scale (generally on the order of nanometer) and the largest scale characterized by the channel size (on the order of centimeter). As pointed out earlier, a popular approach has been to use a local analytical or numerical solution of the Poisson−Boltzmann equation for the double layer region coupled with a numerical solution for the bulk (outside the double layer region). The approach does not consider the effect of the velocity field on the double layer. A direct numerical solution without any simplification has been reported,[22,23] where the geometry is confined to a small length-to-height ratio; hence, direct comparison of these results to experimental data with use of typical channel dimensions of microns (height) × centimeters (length) cannot be made. To overcome this difficulty, we have taken the liquid conductivity in the bulk to be uniform. The deviation of conductivity can be neglected in the case of low surface charge density. Thus, eq 13 may be solved instead of eq 6. Since only one species (the net charge can be treated as a species) is considered, numerical solution can be simplified and the potential distribution along a microchannel centimeters in length can be simulated and compared with our experimental results.

2. Boundary Conditions. For an electrokinetic transport system, different types of boundary conditions exist: inlet, outlet, insulator wall, charged surface, or symmetry axis. Boundary conditions for the Navier−Stokes equations are no-slip conditions on the wall although other slip conditions have also been considered.[26−28] For the Poisson equation, the convection−diffusion−migration equation or the current continuity equation, a prescribed electric potential and species concentrations are imposed on the inlet and outlet. On a charged surface, two kinds of boundary conditions for the electric potential field can be applied: known potential (ζ-potential) or known surface charge density. In this work, a known surface charge density boundary condition is required to solve the governing equations. The normal electric potential relates the charge density as

$$\frac{\partial \phi}{\partial n} = -\frac{\sigma_0}{\epsilon} \tag{14}$$

To ensure electrical neutrality of the entire channel, we employ

$$\sigma_0 + F \sum^{i} Z_i c_i = 0 \tag{15}$$

as a control condition for the convection−diffusion−migration equation or the current continuity equation, where σ_0 is the surface charge density. The fluxes of all species are zero across a symmetry axis or an insulator wall. For a fully developed parallel-plate microchannel flow with the geometry shown in Figure 1, the following boundary conditions are employed:

$$\rho_e = 0,\ \phi = 0, \text{ and } p = p_0 \text{ at } x = 0$$

$$\rho_e = 0,\ \phi = \phi_0, \text{ and } p = 0 \text{ at } x = l$$

$$\frac{\partial \phi}{\partial y} = 0,\ \frac{\partial \rho_e}{\partial y} = 0,\ \frac{\partial u}{\partial y} = 0,\ \frac{\partial v}{\partial y} = 0, \text{ and } \frac{\partial p}{\partial y} = 0 \text{ at } y = 0$$

$$\frac{\partial \phi}{\partial y} = -\frac{\sigma_0}{\epsilon},\ u = v = 0,\ \frac{\partial \rho_e}{\partial y} = 0, \text{ and } \frac{\partial p}{\partial y} = 0 \text{ at } y = a$$

$$\int \sigma_0 \, dx = -\int \int \rho_e \, dx \, dy$$

u and v are velocities in the x and y direction, respectively. The potential difference ϕ_0 across the length is the value of the streaming potential determined experimentally. As the solution of our experiment is deionized-ultrafiltered (DIUF) water, a surface charge density of 1.107×10^{-3} C/m^2 was determined (by means of an experimental ζ-potential of −86 mV) and was used as the boundary condition.

III. Experimental Setup

The experimental system used to study electric potential distribution of a liquid that flows through a parallel-plate microchannel is shown in Figure 2. This system consists of a flow loop, a test section including a slit microchannel, electrodes, instruments for measuring flow and electrokinetic parameters, and a computer acquisition system. The parallel-plate microchannels were assembled by using two identical microscope slides (Fisher Scientific; catalog No. 12-550A) separated by two thin plastic shims (Small Parts Inc., FL) as spacer for the channel walls. The surface roughness of these slides is on the order of 10 nm. The shims were placed along the lateral edges of the

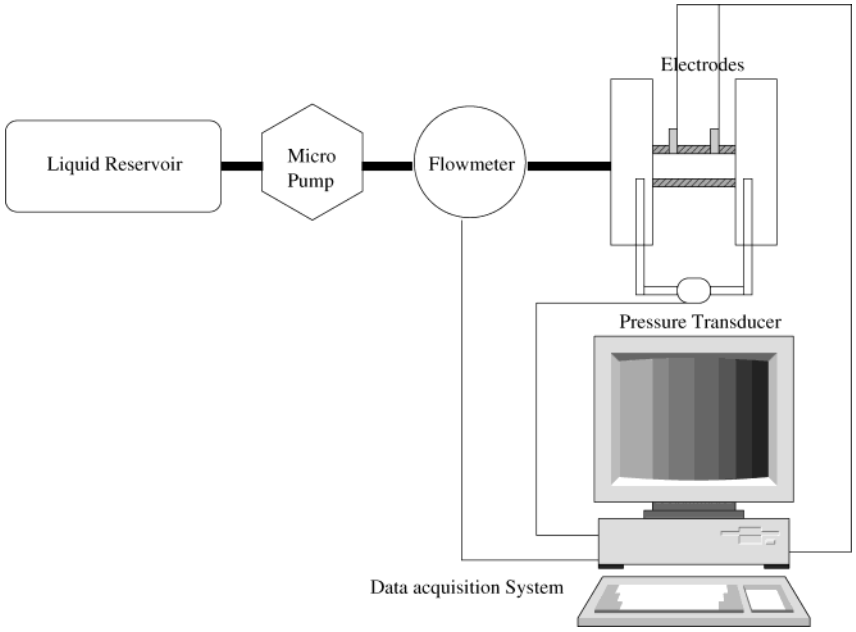

Figure 2. Schematic of the experimental system used to measure the electrokinetic properties of pressure-driven flow in parallel-plate microchannels.

cleaned surfaces and fixed by applying a small amount of epoxy (Devcon, USA), leaving a flow passage 10 mm wide. Once the channel was formed, it was allowed to dry at room temperature for 12 h. Subsequently, the width and the length of the microchannel were measured with use of a precision gauge (Model CD-6″B, Mitutoyo Co., Japan) with an accuracy of ±1 μm. Finally, the microchannel was mounted by two supporting blocks at the inlet and outlet, respectively, to the setup. The channel height was determined by an indirect method that involves measuring a highly concentrated electrolyte flow through the microchannel in a streaming current mode. In this case, the two electrodes used to measure the streaming potential were short-circuited. Therefore, electrokinetic effects can be eliminated; liquid flow is a Poiseuille flow and the channel height can be calculated by the Poiseuille flow equation. The experimental channel height determined by this method is 40 μm.

Before the assembly, four cone-shaped holes were drilled evenly on the upper plate where platinum electrodes are installed. The diameters of the holes on the glass surface are smaller than those of the electrode to ensure that the electrodes do not pass through the upper glass plate and the flow will not be disturbed by the electrodes. Four electrodes were installed evenly onto the upper glass surface. Two other electrodes were inserted near the inlet and outlet into the bulk for streaming potential measurements; this arrangement is identical with typical streaming potential measurements performed in the literature. In the experiment, a pump (LC-5000, ISCO Inc., USA) was set to maintain a constant flow rate. The readings of the pressure drop along the microchannel were monitored and recorded. A high-impedance electrometer (Keithley Instruments Inc., Model 6517A) was used here to measure the electric potentials. The flow was considered to have reached a steady state before measurements of the flow rate, pressure drop, bulk liquid conductivity, and electric potentials along the channel. The data reported in this paper are for steady-state flow. Deionized-ultrafiltered (DIUF) water was selected as our testing liquid for its thicker double layer and smaller κa value, so that the effect of flow field on EDL should become more apparent. For a given channel with DIUF water, the measurements for all the parameters were repeated at least twice for the same flow rate. After the measurements of one flow rate were completed, the pump was set to a different flow rate and the measurements described above were repeated for the same microchannel.

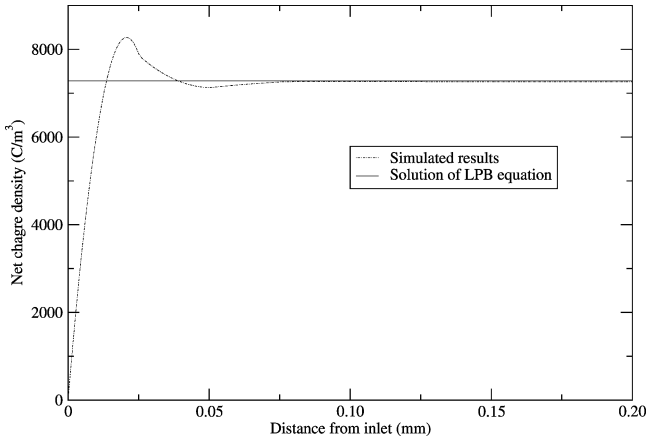

Figure 3. The net charge density distribution at 50 nm away from the wall along the streamwise direction with Re = 6.6.

IV. Results and Discussion

In our study, DIUF water was considered as a binary electrolyte with valences ±1. The concentration was calculated from its conductivity by means of eq 12. The following parameters were taken: $D = 1.0 \times 10^{-9}$ m^2 s^{-1}, $\epsilon = 80 \times 8.854 \times 10^{-12}$ CV^{-1} m^{-1}, $\sigma = 1.0 \times 10^{-4}$ Sm^{-1}. The Debye length (κ^{-1}) calculated from the bulk conductivity of water is 84 nm. Numerical solutions were validated against the analytical solution of the linearized Poisson−Boltzmann (LPB) equation for an equilibrium electrical double layer that is adjacent to an infinitely extended charged surface. The numerical results agreed well with the analytical solutions of the LPB equation without external fields. With the introduction of a flow field, the net charge density distribution will be influenced by the flow field. Figure 3 shows the net charge density distribution at 50 nm away from the wall along the streamwise direction with a Reynolds number (Re) of 6.6. The net charge density distribution follows the solution of the LPB equation on the region far from the inlet. The growth of net charge on the entry region is clearly

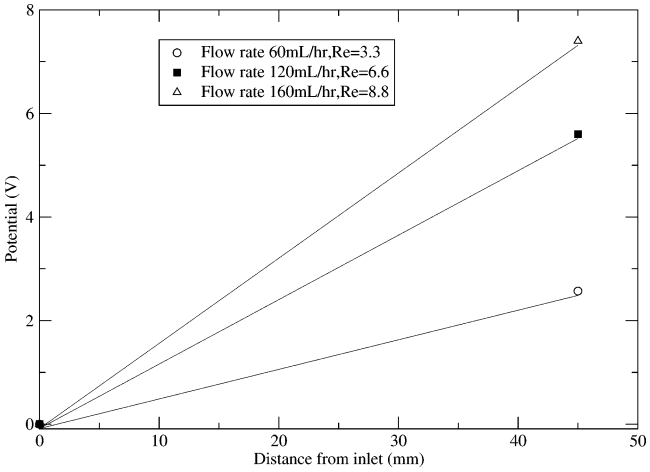

Figure 4. Measured streaming potential at different flow rates for DIUF water. The lines correspond to potential distribution predicted by eq 3. The corresponding Reynolds numbers (Re) are also given.

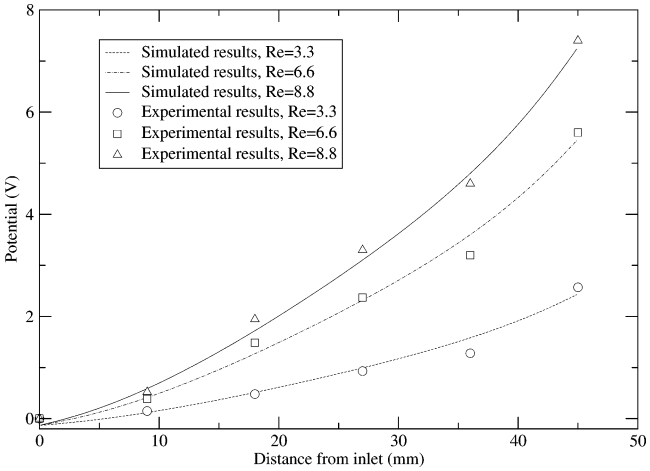

Figure 5. . Comparison of the experimental and simulated potential distribution downstream along a parallel-plate channel of 40 μm (length) $\times$ 10 mm (width) $\times$ 4.5 cm (height) for DIUF water. The simulated results were obtained by the current continuity equation with a charge density of 1.107×10^{-3} C/m^2 as the boundary condition. The corresponding Reynolds numbers (Re) are also given.

demonstrated in Figure 3. Figure 4 displays the measured potentials across the inlet and outlet in the bulk near the surface for three flow rates: 60, 120, and 160 mL/h. Our procedures to determine the streaming potential are consistent with those in the literature by other authors.[13,29,30] The straight lines are predicted potential distribution near the interface along the streamwise direction according to eq 3. If we assume that there is no net charge in the bulk, the lines connecting directly the inlet and outlet potentials in Figure 4 represent the potential distribution in the bulk along the channel. If the distribution is linear, one would also expect those on the surface to follow a straight-line relationship. Figure 5 shows the experimental and simulated potential distribution near the solid−liquid interface along the channel for different flow rates. We see that the measured absolute potential values near the interface do not follow the linear relationship shown in Figure 4; rather, they are nonlinear and smaller than those predicted by eq 3, suggesting that the potential difference between the interface and bulk is larger than that predicted by the Poisson−Boltzmann equation. It should be noted that the three curves in Figure 5 were not curve-fitted, but our simulated results using an experimentally determined charge density of 1.107×10^{-3} C/m^{-2} as the boundary condition. The phenomenon shown in Figures 4 and 5 can be explained as follows.

We start our discussion from the physical mechanism of the streaming potential. On the basis of Helmholtz's theory, the streaming potential is caused by direct movement of electrical charges. However, the continual transfer of electrical charges in liquid does not necessarily cause a potential gradient. This is easily illustrated by the fact that there exists no potential gradient along the channel in the streaming current mode in which the terminal electrodes are short-circuited. In this case, a streaming current will result without any potential difference in the streamwise direction. Hunter[31] stated that accumulation of charges downstream sets up an electric field. If this is true, there must be a charge density gradient in the streaming direction. Hence, we explain the mechanism of streaming potential as follows: at a static state (no flow), ions distribute themselves in EDL as described by the Boltzmann distribution. When a flow field is introduced, hydrodynamic force will drag the diffusion layer downstream. This diffusion layer in EDL near the inlet will be replaced by neutral liquid temporarily. Since charges on the solid surface are immobile, movement of ions in EDL will cause an accumulation of charges downstream and the deficit of counterions upstream temporarily. In this instant, charges on the solid surface upstream and the accumulated charges downstream will draw back counterions and push away coions from the EDL and liquid bulk, in an attempt to recover the initial EDL structure. This effect will cause a migration flux (conduction current) in both streamwise x and height y directions. With respect to the conduction current in the streamwise direction x, a potential difference will result that is the so-called streaming potential. With respect to the conduction current in the height direction y, a potential difference will build up across the channel and the potential at the shear plane is the so-called ζ-potential. When the net current becomes zero, equilibrium is established. The net current then consists of streaming, conduction, and diffusion currents; hence, a steady state is characterized by the equilibrium of these three currents. Thus, the electric field along and across the channel is established by the solid surface charges and the charge redistribution in EDL caused by the streaming current in the channel. In streaming current measurements, on the other hand, since the streaming current at the outlet is conducted back through an outside short-circuit to the entrance, the flow of net charge (streaming current) will not cause similar charge redistribution as in the streaming potential measurements. In streaming current measurements, the electric field in the streamwise direction produced by surface charges is balanced by the electric field resulting from the net charge in EDL. Thus, in the streaming current mode, there is no potential difference in streamwise direction and, hence, we can assume the EDL structure to be the same as the static state.

As described earlier, in the case of streaming potential measurements, a conduction current will be produced in both height y and streamwise x directions by an electric field resulting from solid surface charges and charge redistribution in EDL. If the conduction current in height direction y is different from that in the static state, the potential difference between the EDL and the bulk will be different from that predicted by the Poisson−Boltzmann equation. Figures 4 and 5 indicate that the average conduction current ($|\phi_{sf} - \phi_B|\sigma/a$) in the height direction y in the presence of flow field is much larger than that in the static state. From our previous discussion, we expect that the streaming current is equilibrated by both the diffusion and conduction currents. If the diffusion current is equilibrated

exactly by the conduction current in the height direction y, the streaming current will be equilibrated by the conduction current in the streamwise direction. In this case, the ζ-potential determined from both streaming potential and streaming current methods would be identical. Otherwise, the streaming current will be partially equilibrated by the diffusion and/or conduction currents in the height direction y; the conduction current in the streamwise direction is only a fraction of the streaming current. In the literature, when eq 2 is used to derive the relationship between ζ-potential and streaming potential, the conduction current I_c is considered as the conduction current in the streamwise direction. If the conduction current in the streamwise direction is only a fraction of the streaming current as shown above, the ζ-potential determined from streaming potential and streaming current methods would be different. This discrepancy has frequently been ascribed to the variation of surface conductance by many researchers. From the results presented here, we found that the variation of EDL structure due to flow field may result in the same effect. According to the Poisson equation, the presence of net charge will cause nonlinearity of potential distribution, as confirmed from our experimental results in Figure 5. In this figure, we found that the predicted potential distribution near the interface by numerical simulation agrees reasonably well with those from experiments. When the channel size becomes smaller, we expect that the flow field effect on the EDL structure will be stronger. This flow field effect may explain the unusual behavior of the streaming potential in geometries where the characteristic dimensions are comparable to the Debye length.

V. Conclusions

We have studied the effect of flow field on the electric double layer distribution for a dilute electrolyte (DIUF water) in a streaming potential mode for a 40-μm parallel-plate microchannel. We also measured the electrical potential distribution along the channel near the solid−liquid interface and simulated the distribution by means of a current continuity equation and the Poisson equation. The experimental results show that the average conduction current across the channel with introduction of a flow field is larger than that from the static EDL model for the dilute electrolyte used. The numerical simulation shows that the potential distribution in the streamwise direction in EDL can be nonlinear. Our results indicate that the conduction current in the streamwise direction is only a fraction of the streaming current. Therefore, the ζ-potential values determined from streaming potential measurements are generally smaller than those from streaming current measurements. This discrepancy has frequently been ascribed to the variation of surface conductance and the effect of surface conductance on the streaming potential measurements would have been overestimated when κa is small.

Acknowledgment. We gratefully acknowledge financial support from Canada Research Chair (CRC) Program, Canada Foundation for Innovation (CFI), and Natural Sciences and Engineering Research Council of Canada (NSERC) through a Discovery and a Research Tools and Instrument Grant in support of this research.

References and Notes

(1) Helmholtz, H. *Wied. Ann.* **1879**, *7*, 337.
(2) Gouy, G. *J. Phys.* **1910**, *9*, 457.
(3) Stern, O. *Z. Elektrochem.* **1924**, *30*, 508.
(4) Bull, H. *J. Phys. Chem.* **1935**, *39*, 577.
(5) Dubois, R.; Roberts, A. *J. Phys. Chem.* **1936**, *40*, 543.
(6) Kanamaru, K. *Chem. Abstr.* **1931**, *25*, 3895.
(7) Kim, K.; Fane, A.; M., N.; A., P.; W. R., B.; H., M. *J. Membr. Sci.* **1996**, *116*, 149−159.
(8) Szymczyk, A.; Fievet, P.; Mullet, M.; Reggiani, J.; Pagetti, J. *J. Membr. Sci.* **1998**, *143*, 189−195.
(9) Moyer, L.; Abramson, H. *J. Gen. Physiol.* **1936**, *19*, 727.
(10) Schweiss, R.; Welzel, P. B.; Werner, C.; Knoll, W. *Langmuir* **2001**, *17*, 4304−4311.
(11) Erickson, D.; Li, D.; Werner, C. *J. Colloid Interface Sci.* **2000**, *232*, 186.
(12) Werner, C.; Körber, H.; Zimmermann, R.; Dukhin, S.; Jacobasch, H.-J. *J. Colloid Interface Sci.* **1998**, *208*, 329−346.
(13) Werner, C.; Zimmermann, R.; Kratzmüller, T. *Colloids Surfaces A* **2001**, *192*, 205−213.
(14) White, H.; Urban, F.; Krick, E. *J. Phys. Chem.* **1932**, *36*, 120.
(15) Bull, H.; Gortner, R. *J. Phys. Chem.* **1932**, *32*, 111.
(16) Rutgers, A.; de Smet, M. *Trans. Faraday Soc.* **1945**, *41*, 758.
(17) Patanka, N. A.; Hu, H. *Anal. Chem.* **1998**, *70*, 1870.
(18) Hu, L.; Harrison, J. D.; Masliyah, J. H. *J. Colloid Interface Sci.* **1999**, *215*, 300−312.
(19) Ermakov, S. V.; Jacobson, S. C.; Ramsey, J. M. *Anal. Chem.* **1998**, *70*, 4494.
(20) Mitchell, M. J.; Qiao, R.; Aluru, N. R. *J. Microelectromech. Syst.* **2000**, *9*, 435.
(21) MacInnes, J. M. *Chem. Eng. Sci.* **2002**, *57*, 4539.
(22) Yang, R.-J.; Fu, L.-M.; Hwang, C.-C. *J. Colloid Interface Sci.* **2001**, *244*, 173−179.
(23) Theemsche, A.; Deconinck, J.; Bossche, B. V. D.; Bortels, L. *Anal. Chem.* **2002**, *74*, 4919.
(24) Yang, J.; Masliyah, J. H.; Kwok, D. Y. *Langmuir* **2004**, *20*, 3862−3871.
(25) Wood, L. A. *J. Am. Chem. Soc.* **1946**, *68*, 432−437.
(26) Yang, J.; Kwok, D. Y. *Langmuir* **2003**, *19*, 1047−1053.
(27) Yang, J.; Kwok, D. Y. *J. Micromech. Microeng.* **2003**, *13*, 115−123.
(28) Yang, J.; Kwok, D. Y. *J. Chem. Phys.* **2003**, *118*, 354−363.
(29) Ren, L. Q.; Li, D.; Qu, W. L. *J. Colloid Interface Sci.* **2001**, *233*, 12−22.
(30) Gu, Y.; Li, D. *J. Colloid Interface Sci.* **2000**, *226*, 328.
(31) Hunter, R. *Introduction to Modern Colloid Science*; Oxford University Press Inc.: Oxford, 1993.